Hindawi Publishing Corporation
Science and Technology of Nuclear Installations
Volume 2012, Article ID 312080, 10 pages
doi:10.1155/2012/312080

Research Article

High-Temperature Structural Analysis of a Small-Scale PHE Prototype under the Test Condition of a Small-Scale Gas Loop

Kee-Nam Song,[1] Sung-Deok Hong,[1] and Hong-Yoon Park[2]

[1] *VHTR Technology Development Group, Korea Atomic Energy Research Institute, Daejeon 305353, Republic of Korea*
[2] *AD-Solution Co., Ltd., no. 1101 Hanjin Officetel, 535-5 Bongmyoung-dong, Yuseon-go, Daejeon 305301, Republic of Korea*

Correspondence should be addressed to Kee-Nam Song, knsong@kaeri.re.kr

Received 24 January 2012; Revised 6 May 2012; Accepted 25 June 2012

Academic Editor: Carlo Sborchia

A process heat exchanger (PHE) is a key component for transferring the high-temperature heat generated from a very high-temperature reactor (VHTR) to a chemical reaction for the massive production of hydrogen. The Korea Atomic Energy Research Institute has designed and assembled a small-scale nitrogen gas loop for a performance test on VHTR components and has manufactured a small-scale PHE prototype made of Hastelloy-X alloy. A performance test on the PHE prototype is underway in the gas loop, where different kinds of pipelines connecting to the PHE prototype are tested for reducing the thermal stress under the expansion of the PHE prototype. In this study, to evaluate the high-temperature structural integrity of the PHE prototype under the test condition of the gas loop, a realistic and effective boundary condition imposing the stiffness of the pipelines connected to the PHE prototype was suggested. An equivalent spring stiffness to reduce the thermal stress under the expansion of the PHE prototype was computed from the bending deformation and expansion of the pipelines connected to the PHE. A structural analysis on the PHE prototype was also carried out by imposing the suggested boundary condition. As a result of the analysis, the structural integrity of the PHE prototype seems to be maintained under the test condition of the gas loop.

1. Introduction

Hydrogen is considered a promising future energy solution because it is clean, abundant, and storable and has a high-energy density. One of the major challenges in establishing a hydrogen economy is how to produce massive quantities of hydrogen in a clean, safe, and economical way. Among the various hydrogen production methods, nuclear hydrogen production is gathering attention worldwide since it can produce hydrogen without environmental burden. Research demonstrating the massive production of hydrogen using a very high-temperature reactor (VHTR) designed for operation at up to 950°C has been actively carried out worldwide, including in the USA, Japan, France, and the Republic of Korea (ROK) [1, 2].

The nuclear hydrogen program in the ROK is strongly considering producing hydrogen by employing a Sulfur-Iodine (SI) water-splitting hydrogen production process. An intermediate loop that transports the high heat generated from a nuclear reactor to the hydrogen production process is needed for the nuclear hydrogen program shown in Figure 1. As a component in the intermediate loop, process heat exchanger (PHE) is a kind of heat exchanger that utilizes the high heat from the nuclear reactor to produce hydrogen. PHE is known to be used in several processes such as nuclear steam reforming, nuclear methanol, nuclear steel, and a nuclear oil refinery [2]. The PHE of the SO_3 decomposer, which generates process gases such as H_2, O_2, SO_2, and SO_3, is a key component in the nuclear hydrogen program in the ROK [1, 3].

Recently, the Korea Atomic Energy Research Institute (KAERI) designed and assembled a small-scale nitrogen gas loop for a performance test of VHTR components and manufactured a small-scale PHE prototype made of Hastelloy-X alloy. Nitrogen gas was mainly chosen to make a more efficient use of the blower capacity in the gas loop. A performance test on the PHE prototype is underway in the gas loop, where different kinds of pipelines connecting to the PHE prototype are tested for reducing the thermal stress under the expansion of the PHE prototype. It is known

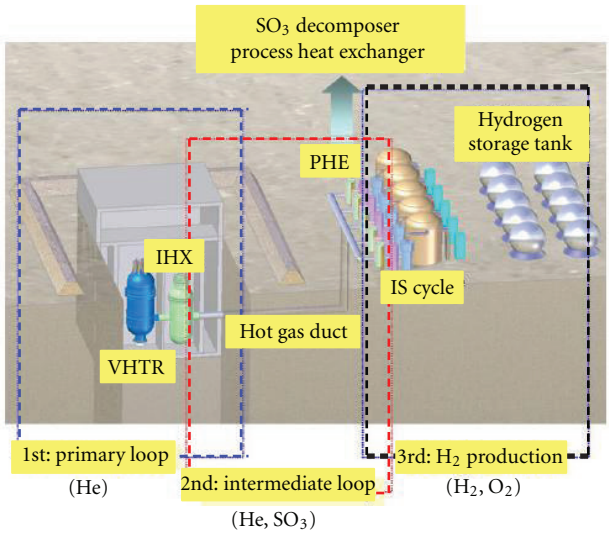

Figure 1: Nuclear hydrogen system.

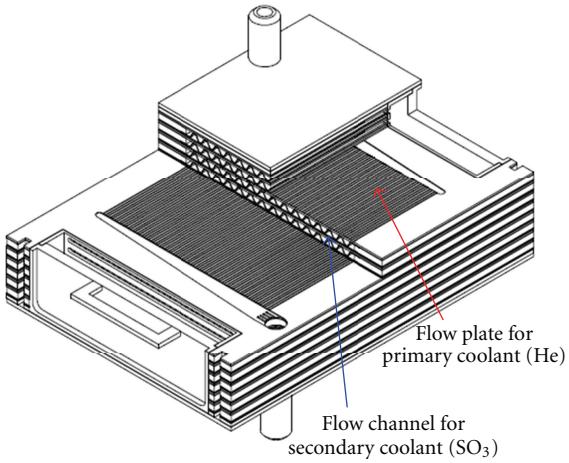

Figure 2: Interior of the PHE.

that the structural boundary condition is very crucial to the structural analysis results of the PHE prototype [4–7]. In this study, to evaluate the high-temperature structural integrity of the PHE prototype under the test condition of the gas loop, a realistic and effective boundary condition imposing the stiffness of the pipelines connected to the PHE prototype is suggested. An equivalent spring stiffness to reduce the thermal stress under the expansion of the PHE prototype was computed from the bending deformation and expansion of the pipelines connected to the PHE. A structural analysis on the PHE prototype has also been carried out by imposing the suggested boundary condition.

2. Finite Element (FE) Modeling

2.1. Structure of the PHE Prototype. A schematic view of the interior of the PHE prototype is illustrated in Figure 2, and detailed shapes of the flow plates for the primary and secondary flows are shown in Figure 3. The PHE

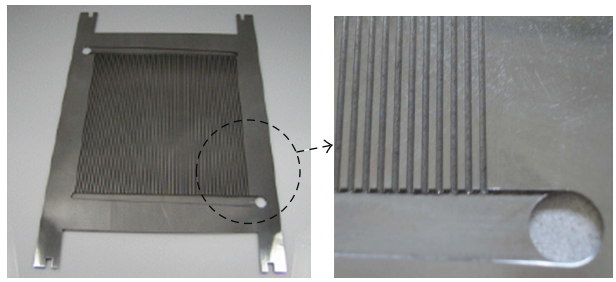

(a) Primary flow plate

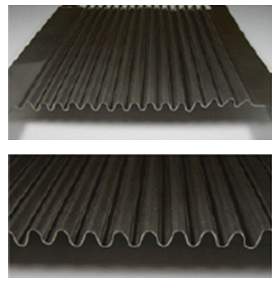

(b) Secondary flow plate.

Figure 3: Flow plates

prototype is designed as a hybrid concept to meet the design pressure requirements between a nuclear system and hydrogen production system. That is to say, the hot gas channel has a compact semicircular shape, similar to a printed circuit heat exchanger, and is designed to withstand the high-pressure difference between loops, while the cold sulfuric acid gas channel has a plate fin shape with sufficient space to install and replace the catalysts for sulfur trioxide decomposition.

All parts of the PHE prototype are made of Hastelloy-X alloy. Grooves of 1.0 mm in diameter are machined into the flow plate for the primary hot coolant shown in Figure 3(a), and waved channels are bent into the flow plate for the secondary cold coolant shown in Figure 3(b). Twenty flow plates for the primary and secondary coolants are stacked on top of each other and are bonded along the edge of the flow plate using a solid-state diffusion bonding method. After stacking and bonding the flow plates, the outside of the PHE is covered with a Hastelloy-X alloy plate 3.0 mm in thickness and is welded along its edges by tungsten inert gas (TIG) welding. A schematic view of the PHE prototype is shown in Figure 4, and a schematic view of the setup of the PHE prototype in the gas loop is shown in Figure 5.

2.2. FE Modeling. Figure 6 shows the overall dimensions and each part of the PHE prototype via 3-D CAD modeling. Based on Figure 6, FE modeling using commercial code I-DEAS was carried out. For the sake of simplicity and understanding the overall behavior of the PHE prototype, the FE model is composed of 911,012 3-D linear solid elements made of 830,304 brick elements, 80,348 wedge elements, and 360 tetrahedron elements.

In the FE model, the inflow/outflow of the primary and secondary coolants are as follows. The inflow of the primary

Table 1: Material properties of Hastelloy-X alloy.

Temperature (°C)	Modulus of elasticity (GPa)	Poisson's ratio	Thermal conductivity (W/m·°C)	Specific heat (J/Kg·K)	Coefficient of thermal expansion (10^{-6}/°C)
20	211	0.3	13.4	419	—
100	206	0.3	14.7	440	11.6
200	201	0.3	16.3	465	12.6
300	194	0.3	—	—	—
400	188	0.3	19.3	515	13.6
500	181	0.3	—	—	—
600	173	0.3	22.5	561	14.0
700	166	0.3	—	—	—
800	149	0.3	25.5	611	15.4
900	148	0.3	—	—	—
1000	141	0.3	28.7	662	16.3

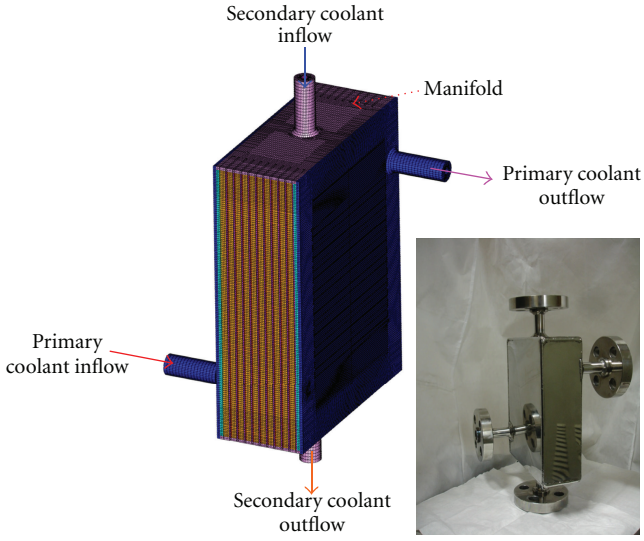

Figure 4: Small-scale PHE prototype.

coolant into the PHE prototype is shown in Figure 7(a). The outflow of the primary coolant from the PHE prototype, after the heat is transferred to the secondary coolant, is shown in Figure 7(b). The inflow of the secondary coolant into the PHE prototype is shown in Figure 8(a). The outflow of the secondary coolant from the PHE prototype, after the heat is received from the primary coolant, is shown in Figure 8(b).

The weld zone including the weld bead (or fusion zone) along the edges of the PHE prototype and the heat affected zone (HAZ) of the inner weld bead of the PHE prototype are also modeled. However, the chamfering (or rounding) along the edge of the PHE prototype is not considered in the FE model for the sake of simplicity. Thus, the stress concentration that occurs around the edges in the FE model will decrease by some degree when considering the real chamfered edges of the PHE prototype.

3. Analysis

3.1. Thermal Analysis. Figure 9 shows the input data of the primary/secondary flow plates for a thermal analysis under a gas loop test condition of 850°C [8]. Table 1 shows the material properties of Hastelloy-X alloy extracted from the website [9]. Based on the input data shown in Figure 9, a thermal analysis on the PHE prototype has been carried out using I-DEAS/TMG Ver. 6.1 [10]. Figure 10 shows the temperature contour of the outside surface of the PHE prototype. The temperature distribution is nearly symmetrical along the vertical axis, and the maximum temperature of the outside surface is about 837.15°C due to external thermal convection and gravity effects.

3.2. Boundary Condition for a Structural Analysis. It was known that structural analysis results depend on the imposed boundary conditions through a series of previous structural analyses on the PHE prototype [4–7]. Therefore, the proper boundary conditions are very crucial to the structural analysis results of the PHE prototype. To evaluate the structural integrity of the PHE prototype installed in the gas loop, it is necessary to impose realistic and effective boundary conditions at the end of the inflow/outflow pipelines connected to the PHE prototype, shown in Figure 5. As illustrated in Figure 5, the PHE prototype, which rests on a fixed stand, is connected with various tubes, such as an U-tube, elbow tube, and straight tubes for the sake of reducing the thermal stress due to the expansion of the PHE prototype under a gas loop test condition. To simulate the boundary conditions properly, the following two points should be considered in the structural analysis of the PHE prototypes: the first point is that the spring stiffness of the pipelines connected to the PHE prototype should be considered, and the second point is that the condition, in which the PHE prototype rests on the fixed stand, should be properly and effectively simulated.

To simulate the first consideration, information on the pipelines connected to the PHE prototype, such as geometric

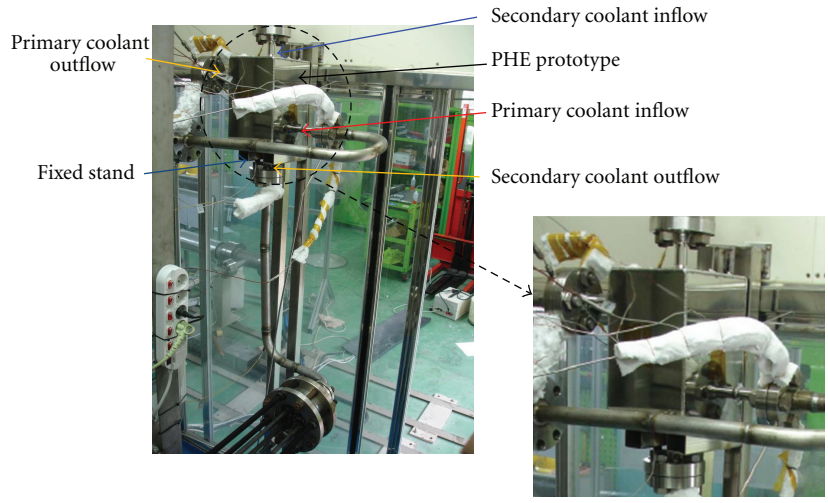

Figure 5: Setup of a PHE prototype in the gas loop.

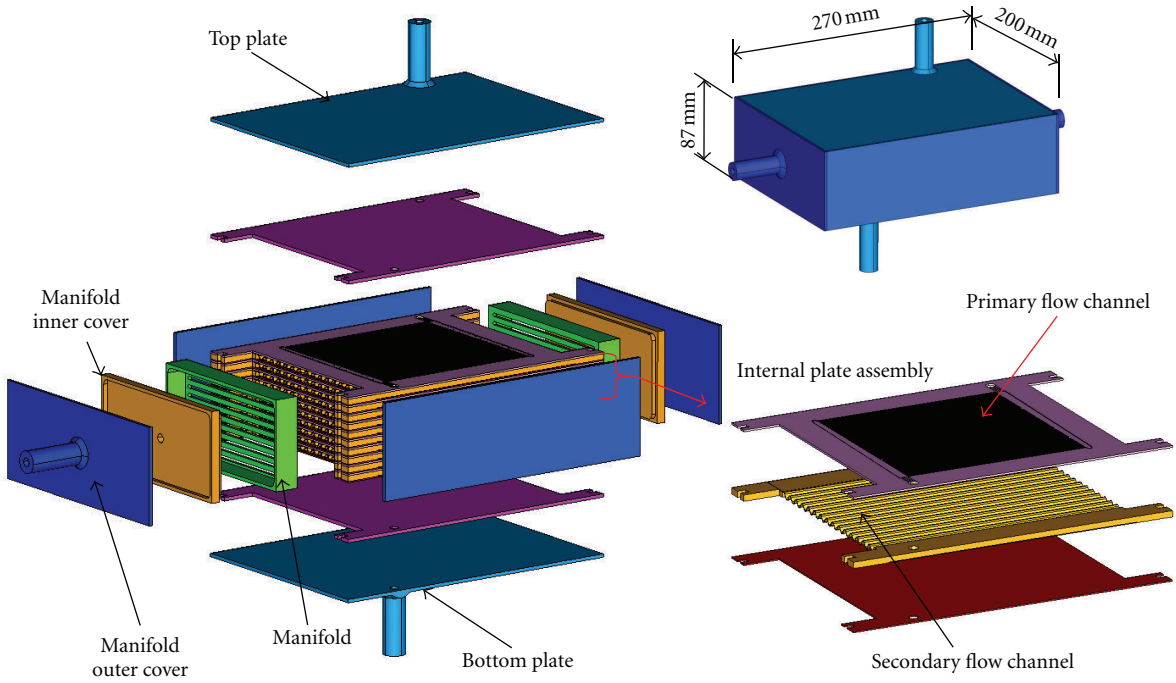

Figure 6: Parts of the PHE prototype.

data and material properties, is needed. To treat the second consideration, a structural analysis on the PHE prototype was first carried out by imposing a contact condition, and realistic and effective boundary condition as a substitute for the contact condition is searched.

3.2.1. Determination of the Spring Stiffness of the Pipelines. Pipelines such as an U-tube and elbow tube can accommodate the thermal expansion under bending deformation, while a straight tube can do it under a linear expansion. In this study, the combined spring stiffness, which comes from the bending deformation and the expansion of the connecting tubes, is imposed as a boundary condition at the end of the inflow/outflow pipelines connected to the PHE prototype. The procedure used to obtain the combined spring stiffness is as follows [11].

The spring stiffness by the expansion of the tubes, k_{ex}, can be obtained from the length (L_{ex}), cross-section area (A), and material elastic modulus (E) of the straight pipeline as follows:

$$k_{ex} = \frac{AE}{L_{ex}}, \tag{1}$$

$$A = \frac{\pi}{4}(D_o^2 - D_i^2), \tag{2}$$

Table 2: Geometric data and spring stiffness of the pipelines.

Location	Material	D_i (mm)	D_o (mm)	L_{ex} (mm)	L_b (mm)	E (GPa)	Kc (N/mm)
Primary coolant inflow ($K_{p\text{-}i}$)	Inc. 800 H	25	34	2850	220	152	1824.9
Primary coolant inflow ($K_{p\text{-}o}$)	Inc. 800 H	20.2	28	1800	250	152	625.9
Secondary coolant inflow/outflow ($K_{s\text{-}i} = K_{s\text{-}o}$)	Hastelloy C-276	25	34	400	200	160.5	2748.2

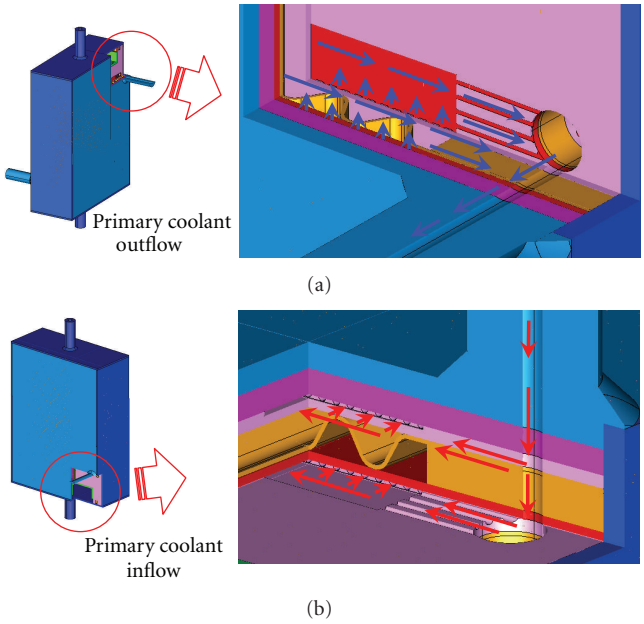

Figure 7: Inflow/outflow of primary coolant.

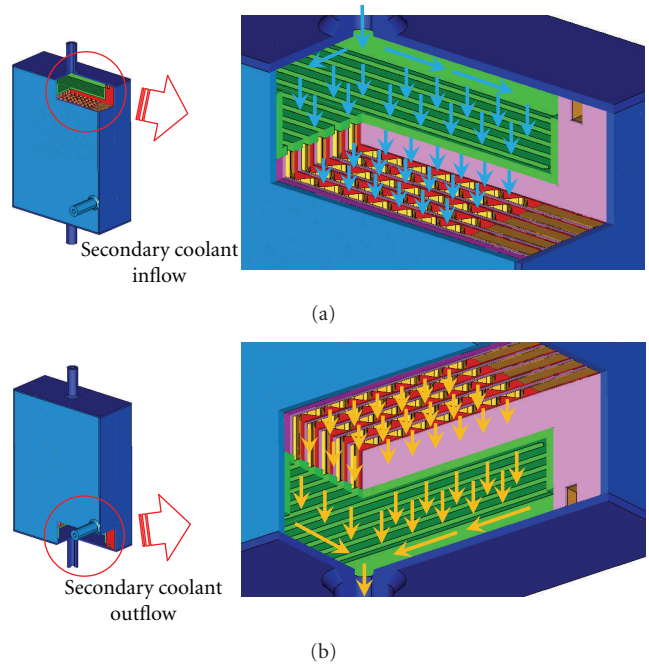

Figure 8: Inflow/outflow of secondary coolant.

where D_o and D_i are the outer and inner diameters of the straight tube, respectively.

The spring stiffness by the bending, k_b, can be obtained from the length of the arm for the bending deformation (L_b), the second moment of the pipe cross-section area (I_b), and the material elastic modulus of the U-tube or elbow tube as follows [11]:

$$k_b = \frac{3EI_b}{L_b^3}, \tag{3}$$

$$I_b = \frac{\pi}{64}(D_o^4 - D_i^4). \tag{4}$$

when the pipelines connected to the PHE prototype are combined by straight tubes, U-tubes, and elbow tubes, the combined spring stiffness, k_c, can be obtained by a parallel connection of the expansion springs and bending springs as follows [11]:

$$\frac{1}{k_c} = \frac{1}{k_{ex}} + \frac{1}{k_b}. \tag{5}$$

Table 2 shows the geometric data, material properties of pipelines connected to the PHE prototype, and the equivalent spring stiffness using (1)–(5). Table 3 shows the mechanical properties of Hastelloy-X alloy extracted from the Hastelloy-X alloy website [9].

3.2.2. Modeling of Contact Condition. The PHE prototype in the gas loop rests on a fixed stand as shown in Figure 5. Thus, contact conditions should be imposed on the bottom surface of the PHE prototype in the FE model for a realistic structural analysis. Figure 11 shows a modeling of the contact condition at the bottom surface of the PHE prototype, in which the fixed stand, composed of a pair of square hollow beams 2.0 mm thick, is modeled by two supporting cantilevers, and a friction coefficient of 0.1 is used to avoid an excessive sliding of the PHE prototype on the contact surface.

3.3. Structural Analysis. Several kinds of structural analyses on the PHE prototype were carried out using the commercial code ABAQUS Ver. 6.8 [12], that is, one analysis by imposing the contact condition shown in Figure 11, and another analyses by imposing several alternative boundary conditions by removing the contact condition to reduce substantially the computing time to get the analysis results [13].

3.3.1. Structural Analysis Imposing the Contact Condition. Figure 12 shows the stress contour from the structural analysis imposing the contact condition. According to Figure 12, even the maximum stress of 310.0 MPa which occurs near the contact area of the corner of the supporting beam

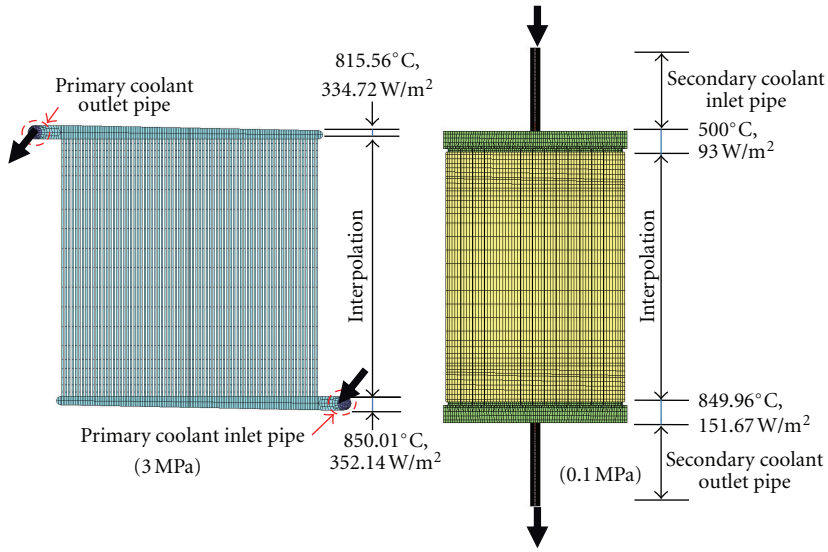

Figure 9: Boundary condition of primary/secondary coolant.

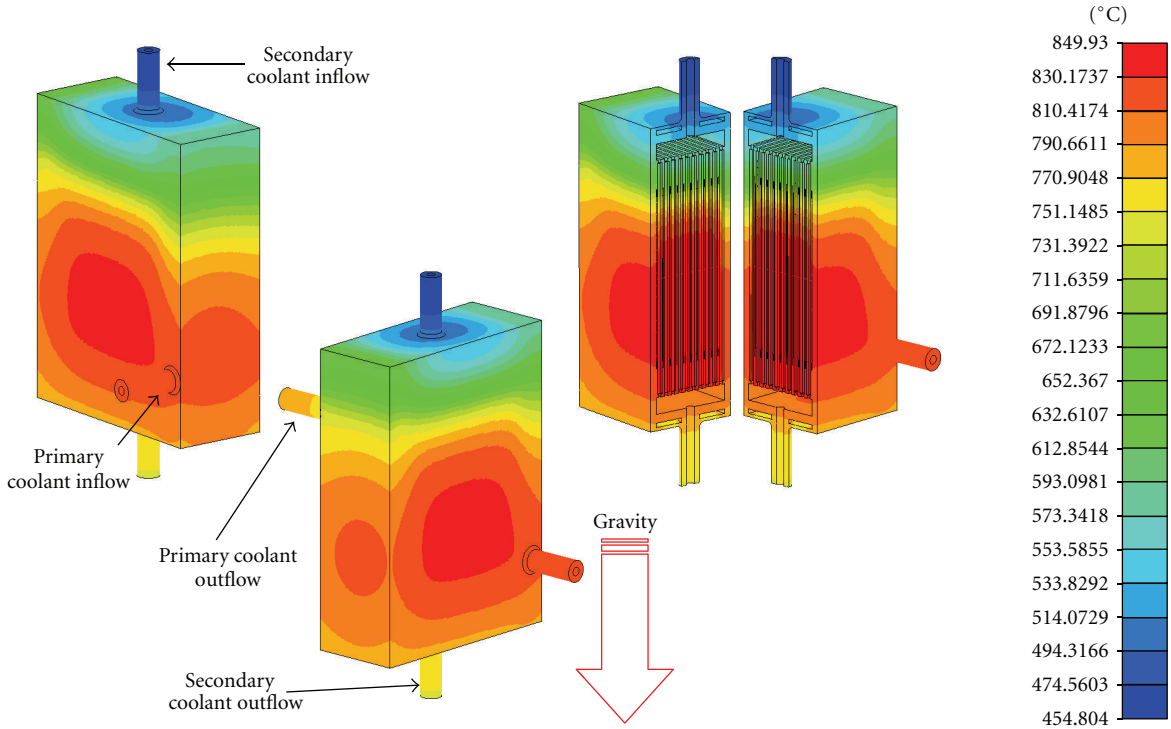

Figure 10: Temperature contour of the PHE outside surface.

exceeds the yield stress of Hastelloy-X alloy (233.5 Mpa at 767°C), this maximum stress is not important from the viewpoint of structural integrity, as the maximum stress occurs locally in a very small and narrow region. However, the structural analysis imposing the contact condition is not efficient enough to obtain the analysis results, as it requires too much computing time, such as 5 days even with the IBM P6 GAIA of a supercomputer. Thus, searching for a substitute for the contact condition is needed for an efficient structural analysis of the PHE prototype. Figure 13 shows the strain contour from the structural analysis imposing the contact condition, which implies effective substantial information to search for a substitute for the contact condition in the following subsection.

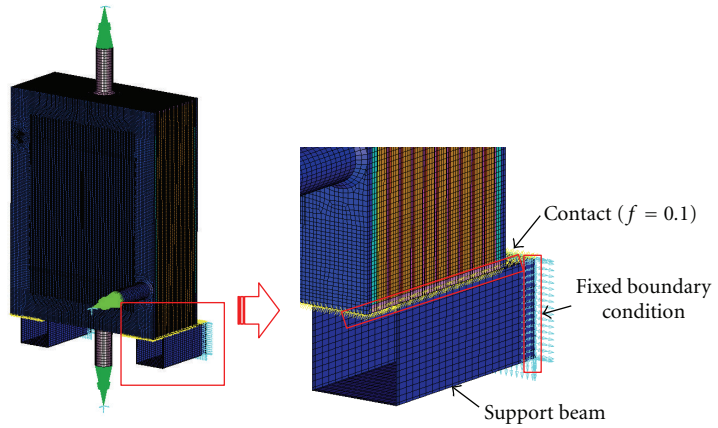

Figure 11: Contact condition.

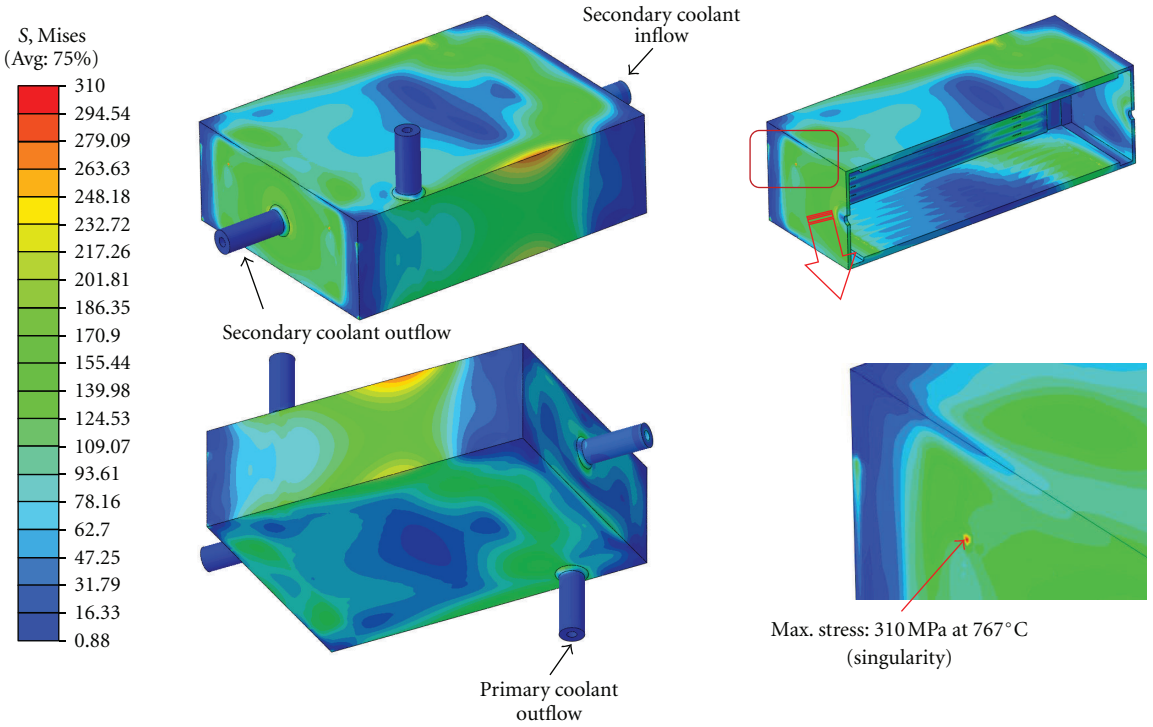

Figure 12: Stress contour in case of imposing contact condition.

Table 3: Mechanical properties of Hastelloy-X alloy.

Form	Condition	Average tensile data*						
		Test temperature		Ultimate tensile strength		Yield strength at 0.2% offset		Elongation in 2 in. (50.8 mm)
		°F	°C	Ksi	MPa	Ksi	MPa	%
Sheet 0.045–0.060 in. (1.1–1.5 mm) thick	Bright annealed at 2150°F (1177°C), hydrogen cooled	Room		111.2	767	54.9	379	44
		1000	538	89.0	614	35.6	245	49
		1200	649	84.2	581	35.4	244	54
		1400	760	67.1	463	34.4	237	53
		1600	871	44.9	310	28.1	194	59
		1800	982	25.6	177	13.2	91	66
		2000	1093	14.0	97	6.3	43	60

* Strain rate was 0.005-inch/inch/minute to 0.2% yield point and 0.5-inch/inch/minute to failure.

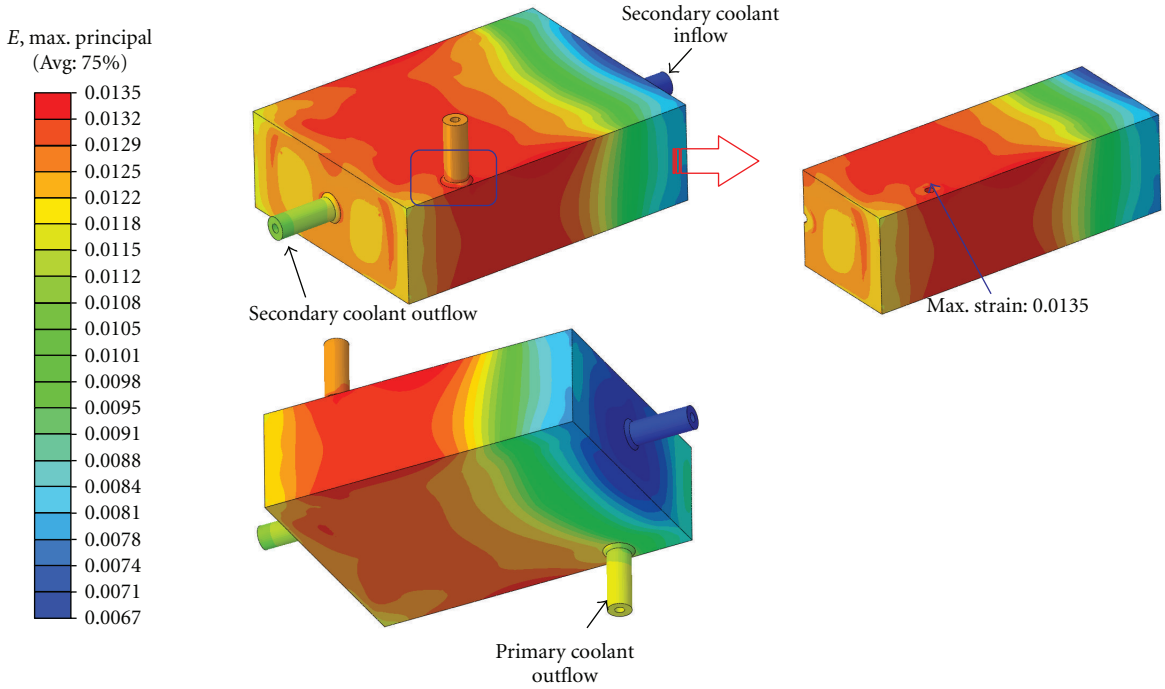

Figure 13: Strain contour in case of imposing contact.

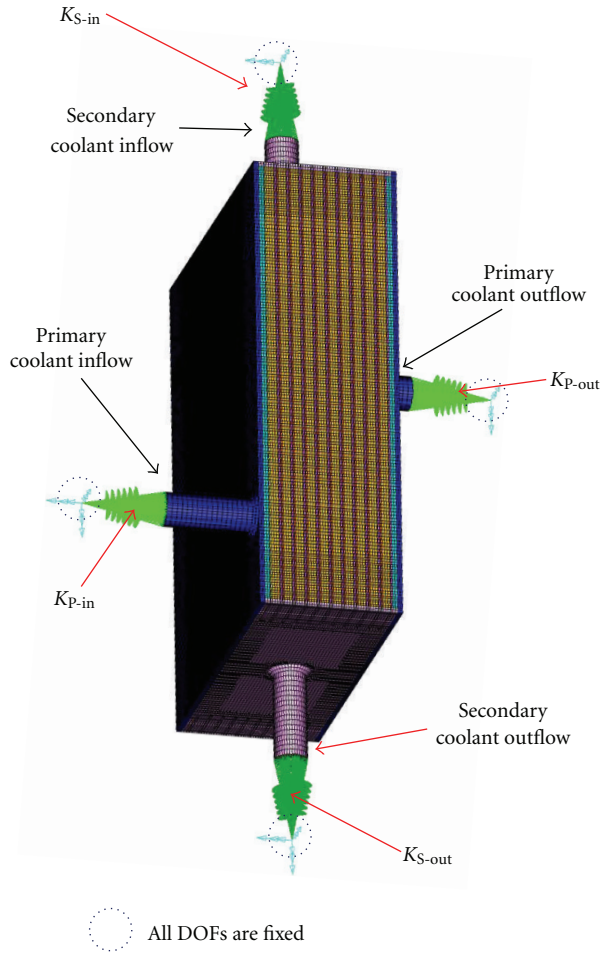

Figure 14: Suggested boundary condition.

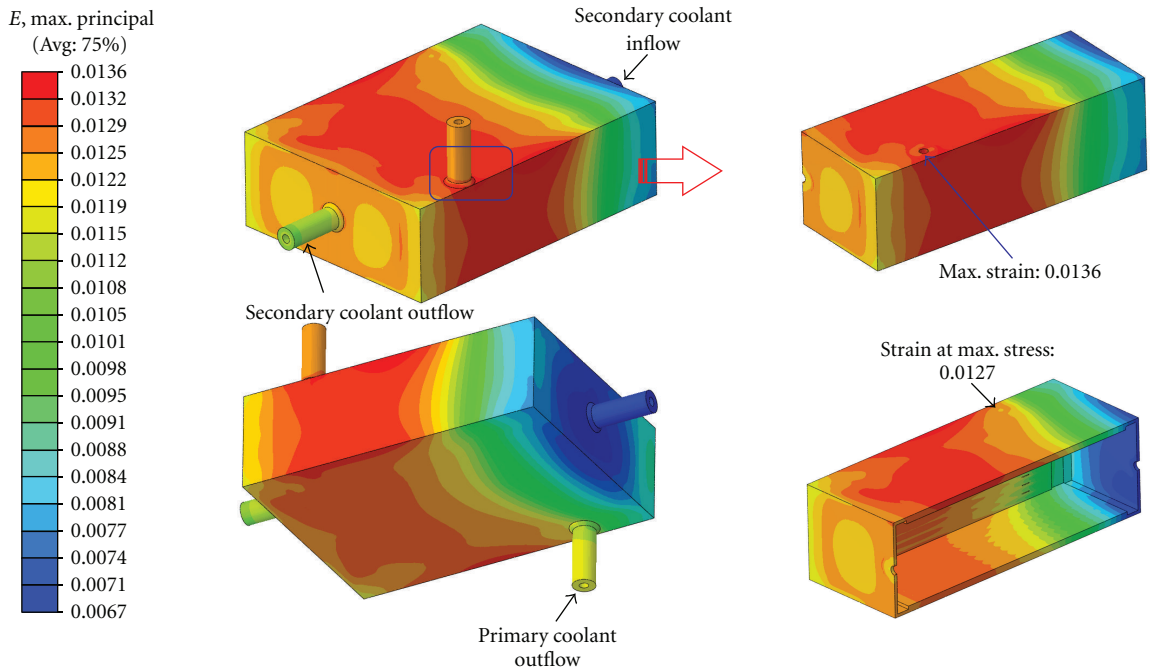

Figure 15: Strain contour in case of imposing a suggested boundary condition.

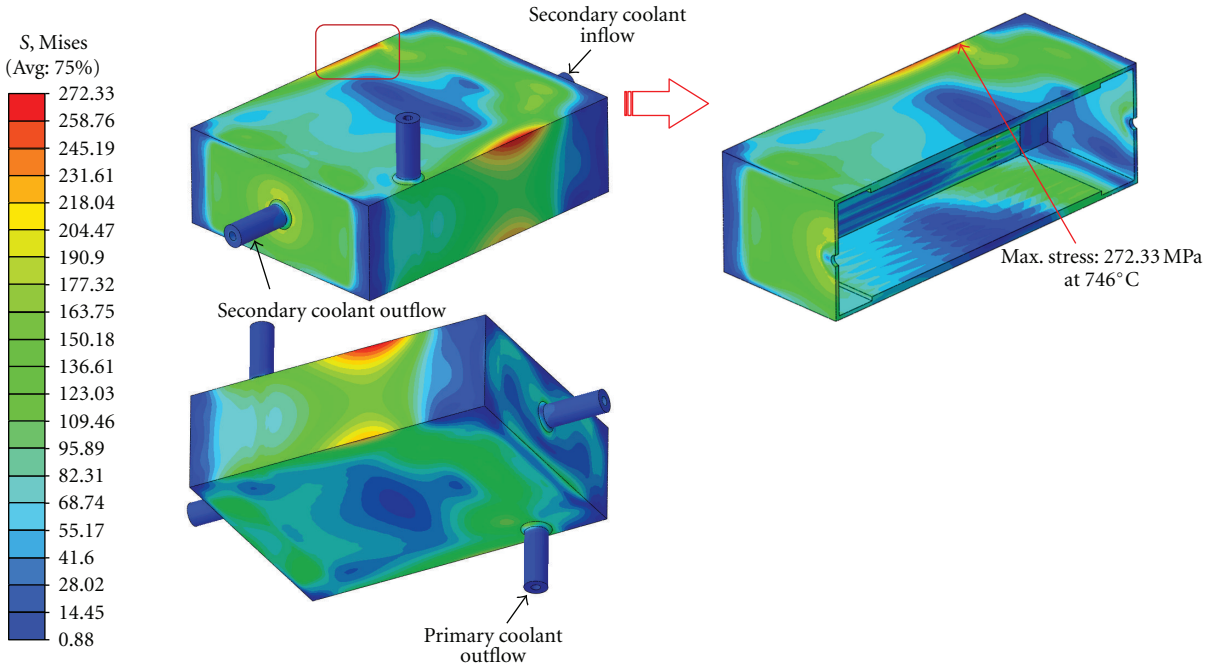

Figure 16: Stress contour in case of imposing a suggested boundary condition.

3.3.2. Structural Analysis Imposing an Alternative Condition. Through a series of structural analyses imposing alternative boundary conditions [13], an efficient substitute for the contact condition is suggested as follows. Figure 14 shows an efficient substitute for the contact condition, and the computing time imposing the suggested boundary condition is only about 4 hours even with the Z800 workstation. Figure 15 shows the strain contour from the structural analysis imposing an efficient substitute for the contact condition shown in Figure 14. According to Figure 15, the strain contour, which supplies information on the deformed shape of the PHE prototype, is nearly the same as that shown in Figure 13, which means that the substituted condition seems to be an effective and proper boundary condition for the structural analysis of the PHE prototype.

Table 4 shows the mechanical properties of Hastelloy-X alloy in the weld zone [14]. Figure 16 shows the stress contour of the PHE prototype from the structural analysis

Table 4: Normalized mechanical properties of Hastelloy-X alloy in the weld zone.

	Yield stress	Ultimate tensile strength
Base material	1.000	1.000
Heat-affected zone	0.962	0.998
Weld zone	1.094	1.120

imposing the efficient substitute for the contact condition shown in Figure 14. According to Figure 16, the maximum local stress of 273.33 MPa occurs on the edge of the top plate, that is, in the weld zone, which exceeds the yield stress of the weld material of Hastelloy-X (269.5 MPa) [9, 14] by only 1.0%. Since the edges of the PHE prototype are in reality chamfered, the maximum local stress will decrease to a certain extent when considering the chamfered edges. Therefore, the high-temperature structural integrity of the PHE prototype seems to be guaranteed in the gas loop test condition.

4. Conclusions

To evaluate the high-temperature structural integrity of the PHE prototype under the test condition of the gas loop, a structural analysis on the PHE prototype including FE modeling and thermal analysis was carried out. As a result of this analysis, we drew the following conclusions.

(1) A boundary condition, considering the bending deformation and the expansion of the pipelines connected to the PHE prototype and substituting the contact condition, was suggested.

(2) The strain contour obtained by imposing the contact condition is nearly the same as that by imposing the suggested boundary condition.

(3) The suggested boundary condition seems to be a realistic and effective boundary condition for the structural analysis as a substitute for the contact condition.

(4) Considering the chamfering effect on the edges of the PHE prototype, the structural integrity of the prototype seems to be guaranteed.

References

[1] J.-H. Chang, Y.-W. Kim, K.-Y. Lee et al., "A study of a nuclear hydrogen production demonstration plant," *Nuclear Engineering and Technology*, vol. 39, no. 2, pp. 111–122, 2007.

[2] W. J. Lee, Y. W. Kim, and J. H. Chang, "Perspectives of nuclear heat and hydrogen," *Nuclear Engineering and Technology*, vol. 41, no. 4, pp. 413–426, 2009.

[3] Y. Shin, J. Chang, J. Kim et al., "A dynamic simulation of the sulfuric acid decomposition process in a Sulfur-Iodine nuclear hydrogen production plant," *Nuclear Engineering and Technology*, vol. 41, no. 6, pp. 831–840, 2009.

[4] K. N. Song, H. Y. Lee, C. S. Kim, S. D. Hong, and H. Y. Park, "High-temperature structural-analysis model of process heat exchanger for helium gas loop (I)," *Transactions of the Korean Society of Mechanical Engineers A*, vol. 34, no. 9, pp. 1241–1248, 2010.

[5] K. N. Song, H. Y. Lee, C. S. Kim, S. D. Hong, and H. Y. Park, "High-temperature structural analysis model of the process heat exchanger for helium gas loop (II)," *Transactions of the Korean Society of Mechanical Engineers A*, vol. 34, no. 10, pp. 1455–1462, 2010.

[6] K. N. Song, S. D. Hong, and H. Y. Park, "High-temperature structural analysis of a small-scale prototype of a process heat exchanger (IV)—macroscopic high-temperature elastic-plastic analysis," *Transactions of the Korean Society of Mechanical Engineers A*, vol. 35, no. 10, pp. 1249–1255, 2011.

[7] K. N. Song, J. H. Kang, S. D. Hong, and H. Y. Park, "Elastic high-temperature structural analysis on the small-scale PHE prototype considering the pipeline stiffness," *Transactions of the Korean Society of Pressure Vessels and Piping*, vol. 7, no. 3, pp. 48–53, 2011.

[8] K. N. Song, H. Y. Lee, C. S. Kim, S. D. Hong, and H. Y. Park, "High-temperature structural analysis of small-scale prototype of process heat exchanger (III)," *Transactions of the Korean Society of Mechanical Engineers A*, vol. 35, no. 2, pp. 191–200, 2011.

[9] Hastelloy-X alloy, http://www.haynesintl.com/pdf/h3009.pdf, June 2012.

[10] Siemens PLM Software I-DEAS/TMG User Manual Version 6.1, 2009.

[11] S. H. Crandall, N. C. Dahl, and T. J. Lardner, *An Introduction to the Mechanics of Solid*, McGraw-Hill Kogakusha, Tokyo, Japan, 1972.

[12] Dassault Systemes Simulia ABAQUS User Manual Version 6.8, 2009.

[13] K. N. Song, S. D. Hong, and H. Y. Park, "High-Temperature structural analysis on the small-scale PHE prototype under the test condition of small-scale gas loop," *Transactions of the Korean Society of Pressure Vessels and Piping*, vol. 8, no. 1, pp. 1–7, 2012.

[14] K. N. Song and D. S. Ro, "Measurement of mechanical properties in weld zone of nuclear material using an instrumented indentation technique," *Journal of the Korean Welding and Joining Society*, vol. 30, no. 3, pp. 249–254, 2012.